

# Glucose-Based Molecular Rotors as Fluorescent Inhibitors and Probes of Glycogen Phosphorylase <sup>†</sup>

Konstantinos F. Mavreas <sup>1</sup>, Michael Mamais <sup>1,2</sup>, Panagiota Papazafiri <sup>2</sup> and Thanasis Gimisis <sup>1,\*</sup>

<sup>1</sup> Department of Chemistry, National and Kapodistrian University of Athens, 15771 Athens, Greece; kmavreas@chem.uoa.gr (K.F.M.); mmamais@chem.uoa.gr (M.M.)

<sup>2</sup> Department of Biology, National and Kapodistrian University of Athens, 15771 Athens, Greece; ppapaz@biol.uoa.gr

\* Correspondence: gimisis@chem.uoa.gr

<sup>†</sup> Presented at the 24th International Electronic Conference on Synthetic Organic Chemistry, 15 November–15 December 2020; Available online: <https://ecsoc-24.sciforum.net/>.

**Abstract:** In this study, (*E*)-2-cyano-3-(6-(dimethylamino)naphthalen-2-yl)-*N*-( $\beta$ -D-glucopyranosyl)acrylamide, a  $\beta$ -D-glucopyranosyl analogue of the widely used molecular rotor julolidine, was synthesized and studied photochemically. The new compound is a fluorescent inhibitor of rabbit muscle glycogen phosphorylase with properties of a molecular rotor. Fluorescence measurements in solutions of increasing viscosity determined that the fluorescence intensity increases with the viscosity of the medium, indicating that the new compound exhibits molecular rotor characteristics. Although the compound fluoresces negligibly in an aqueous buffer solution, in the presence of increasing amounts of rabbit muscle glycogen phosphorylase, we observed an increase in fluorescence intensity, which was attributed to the formation of an inhibitor–enzyme complex. In-vitro cellular studies were also undertaken, yielding promising preliminary results for the use of the new compound as a fluorescent probe.

**Keywords:** molecular rotor; glycogen phosphorylase; julolidine; fluorescent probes

**Citation:** Mavreas, K.F.; Mamais, M.; Papazafiri, P.; Gimisis, T. Glucose-Based Molecular Rotors as Fluorescent Inhibitors and Probes of Glycogen Phosphorylase. *Chem. Proc.* **2021**, *3*, 45. <https://doi.org/10.3390/ecsoc-24-08414>

Academic Editors: Julio A. Seijas and M. Pilar Vázquez-Tato

Published: 14 November 2020

**Publisher's Note:** MDPI stays neutral with regard to jurisdictional claims in published maps and institutional affiliations.



**Copyright:** © 2020 by the authors. Licensee MDPI, Basel, Switzerland. This article is an open access article distributed under the terms and conditions of the Creative Commons Attribution (CC BY) license (<http://creativecommons.org/licenses/by/4.0/>).

## 1. Introduction

Glycogen phosphorylase (GP) is an enzyme that plays a key role in glucose homeostasis. The lack of proper GP regulation is involved in a number of pathological states such as type 2 diabetes [1,2] and cancer [3–6], while recent findings connect GP to Alzheimer's disease and a number of other neurological disorders [7,8]. The ubiquitous presence of GP has ascended the design and synthesis of GP activity-modulating agents into an exciting field in chemical research in recent years. Our team has been working on the synthesis and study of potential GP inhibitors, with the creation of new agents to be used against type 2 diabetes as the main aim [9–11].

Molecular rotors are conditionally fluorescent compounds, which contain two or more chromophores in a push–pull configuration. When the chromophores are forced to be aligned parallelly, the compounds fluoresce. If the system is free to rotate, it forms twisted intramolecular charge transfer (TICT) states, the excited state decays thermally, and no fluorescence is observed (Figure 1). These fluorescence characteristics are strongly affected by particular microenvironments [12,13]. Molecular rotors show an enhancement in their fluorescence with increasing viscosity of the surroundings, as well as during binding to protein targets in cells. Compounds with molecular rotor functions, such as  $\alpha$ -cyanoacryl-derivatives of julolidine (Figure 1), have been applied as biosensors to determine the viscosity in various cellular microenvironments [14–16].

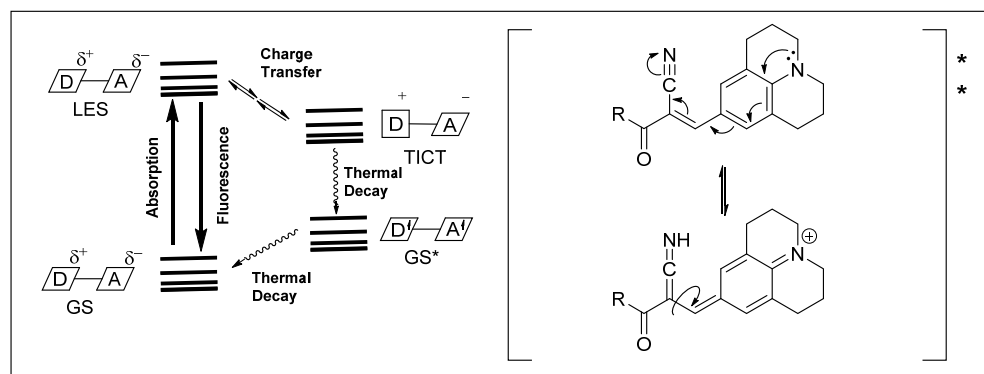


**Figure 1.** Mechanism of induced fluorescence in  $\alpha$ -cyanoacryl-derivatives of julolidine via twisted intramolecular charge transfer states (TICTs).

Compounds that exhibit selective fluorescence upon binding to the catalytic site of GP could be potentially useful fluorescent probes, allowing a better understanding of glycogen metabolism by using fluorescence microscopy. Herein, the first attempts to extend our work to the synthesis of glucose-based GP ligands with attached moieties acting as molecular rotors, are described.

## 2. Results and Discussion

Based on our previous experience with the synthesis of GP  $N^4$ -arylamine-substituted 1-( $\beta$ -D-glucopyranosyl)pyrimidin-2-one inhibitors, we set out to design an  $N$ -glycoside incorporating a molecular rotor moiety. More specifically, it was decided to use the (*E*)-2-cyano-3-(6-(dimethylamino)naphthalen-2-yl)acryl-moiety [17,18], which has been shown to exhibit the desired molecular rotor characteristics, attached to a  $\beta$ -D-glucopyranose by means of an amide bond. The proposed aglycon was expected to satisfactorily mimic the structural characteristics of molecules (previously synthesized by our group [9–11]) necessary to strongly bind to the catalytic site of rabbit muscle glycogen phosphorylase (RMGP) (Figure 2). Furthermore, use of the dimethylaminonaphthyl-system was expected to lead to compounds with excitation and emission maxima falling within the region of the filter-sets commonly used in fluorescence microscopy for the observation of the mCherry fluorescent protein (450–600 nm for excitation and 600–700 nm for emission) [19]. The same chromophore system has also been utilized as a two-photon fluorescent sensor for near-infrared imaging in whole tissues [17,18].

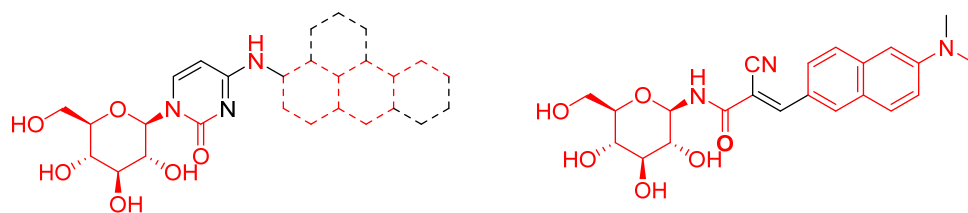
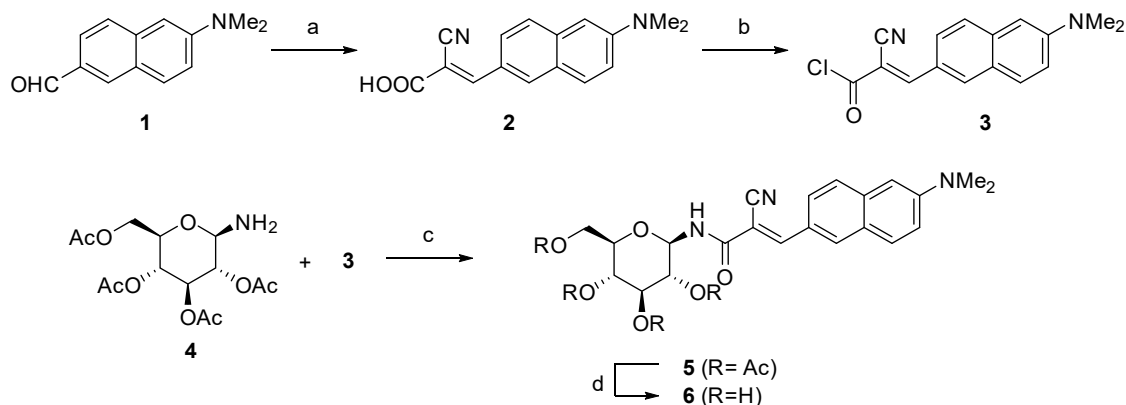


**Figure 2.** Structural comparison between the general framework of previously synthesized 4-arylamine-substituted 1-( $\beta$ -D-glucopyranosyl)pyrimidin-2-one GP inhibitors (left) and the proposed compound (right).

The synthesis started with the preparation of known 6-dimethylamino-2-naphthaldehyde (**1**) from commercially available  $\beta$ -naphthol, following previously published procedures [20,21]. Utilizing the Knoevenagel condensation with cyanoacetic acid [22], aldehyde (**1**) was transformed into the corresponding acid (**2**, Scheme 1) in a 90% yield. It was then attempted to couple the acid (**2**) with 2,3,4,6-tetra-*O*-acetyl- $\beta$ -D-glucopyranosylamine (**4**) [23,24]. Initially, this was done with methodologies utilizing carbodimide reagents (DCC and EDC), but this approach failed to produce the desired amide. Alternatively,

transformation of the acid (**2**) into the corresponding acid chloride (**3**), by use of oxalyl chloride, was successful. The crude chloride (**3**) was then reacted with the amine (**4**) to yield the desired amide (**5**) as a component of an inseparable mixture. The crude mixture was directly submitted to deprotection, using methanolic ammonia, to remove the acetyl groups. The final compound (**6**) was successfully isolated by column chromatography, albeit in moderate 35 % yield, over three steps starting from the acid (**2**).



**Scheme 1.** (a) Piperidine, cyanoacetic acid in MeCN, 80 °C, 12 h, 90%; (b) oxalyl chloride, cat. DMF in DCM, r.t., 1 h; (c) 3, pyridine, r.t., 2 h; (d) NH<sub>3</sub> in MeOH, 24 h, 35% over three steps.

Subsequently, the spectroscopic properties of compound (**6**) were studied in solution. In a DMSO solution, (**6**) exhibited a  $\lambda_{\text{max}}$  at 427 nm ( $\epsilon = 29,500 \text{ cm}^{-1}\text{M}^{-1}$ ). A red shift of  $\Delta\lambda \approx 10 \text{ nm}$ , with increasing concentrations from 1 to 75  $\mu\text{M}$ , was observed. Excitation at the  $\lambda_{\text{max}}$  led to emission as a broad peak, centered at 580 nm. The absorption spectra in solutions of diethylene glycol: glycerol (DEG:Gl) of increasing viscosity (100% DEG, 50% DEG:Gl, 100% Gl, Figure 3) exhibited a  $\lambda_{\text{max}} \approx 450 \text{ nm}$ , and a similar red shift was observed going from low to high viscosity. Excitation of the above solutions at the  $\lambda_{\text{max}}$  led to variable fluorescence correlating well with the solution viscosity. Specifically, a 60-fold increase in viscosity led to a four-fold increase in the fluorescence intensity, confirming that (**6**) exhibits the expected properties of a molecular rotor.

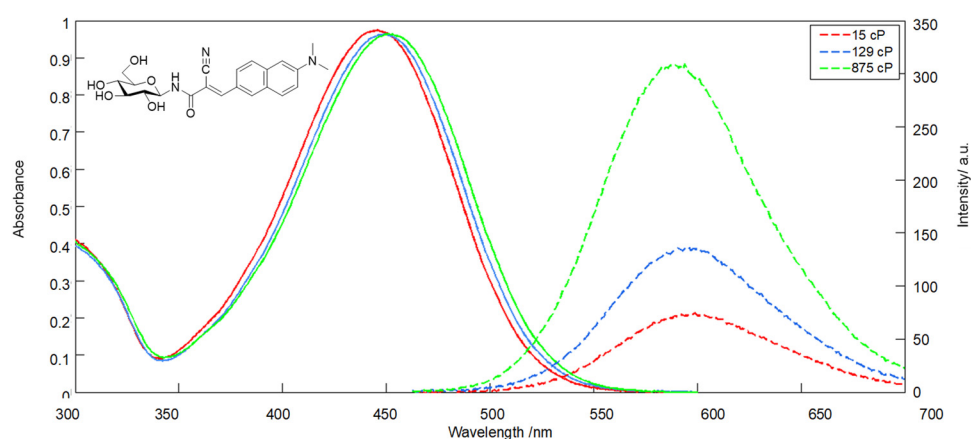


**Figure 3.** Absorption (left) and emission (right) spectra of (**6**) in relation to solution viscosity (red: 100% Gl,  $\mu = 15 \text{ cP}$ ; blue: 50% diethylene glycol: glycerol (DEG:Gl),  $\mu = 129 \text{ cP}$ ; green: 100% DEG,  $\mu = 875 \text{ cP}$ ).

Having proven the molecular rotor behavior of (**6**), the next step was to study its interaction with rabbit muscle glycogen phosphorylase. A number of RMGP:(**6**) ratios in

the range 0–10 were used to ensure maximal ligand binding to the enzyme. The experiments were performed in the suitable assay buffer ( $\beta$ -glycerophosphate 2.5 mM, 2-mercaptoethanol 2.5 mM, EDTA 0.05 mM) commonly used with RMGP. During the first set of experiments, the only visible effect was the flattening of the absorption spectrum of (6), regardless of the enzyme's concentration (results not shown). Absorption spectra of (6) under a variety of pH levels were examined (Figure S5), which ascertained the compound's stability at the pH of the assay buffer (6.8) used in the experiments with RMGP. As shown in Figure S5, compound (6) exhibited the same absorption spectral characteristics in the 6.1–8.9 pH region. For this reason, we tried to attribute the observed spectral changes of (6) in the assay buffer to the buffer's constituents as a source of possible interference. Structurally related  $\alpha$ -cyanoacrylamide systems have been previously shown to exhibit a propensity to undergo 1,4 addition with thiols [25], which seemed to be the case with (6). Repeating the experiments in a modified assay buffer, excluding the usually added 2-mercaptoethanol, led to results similar to the previously obtained spectra of (6) with a  $\lambda_{\max} \approx 450$  nm, which blue-shifted with increasing amounts of RMGP (Figure 4). At the maximum RMGP concentration (RMGP:(6) ratio of 10:1), fluorescence was enhanced three times compared to the fluorescence of free (6) in the 2-mercaptoethanol-free aqueous buffer solution (Figure 4).

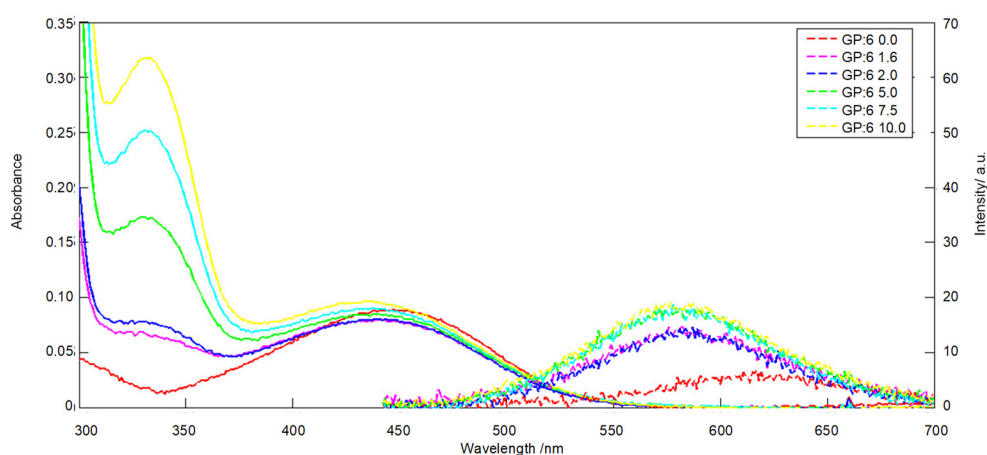


**Figure 4.** Absorption (left) and emission (right) spectra of RMGP:(6) complex in rising ratios of RMGP.

The above experiments established that (6) behaves as a molecular rotor upon binding to the catalytic site of RMGP. The same fluorescence assays were repeated using bovine serum albumin to exclude possible generic interactions as well as with hexokinase III, an enzyme which is a possible target for the binding of glucose-based molecules. In both cases, there was no enhancement of fluorescence witnessed. Although these results are preliminary, they strongly indicate that (6) binds to RMGP in a target-specific fashion. There was a smaller enhancement of fluorescence in the presence of RMGP when compared to the one observed in solutions of increasing viscosity. This could be either due to weaker than expected binding of (6) to RMGP or due to a fluorescence quench by the residues lining up the catalytic site of RMGP. The exact reasons may be elucidated upon further kinetic and crystallographic studies.

In the final step of this study, some preliminary fluorescence microscopy experiments were performed. The A-431 and Hep2G cell lines were selected, since both are known to express high levels of the liver isoform of GP (PYGL) [26], which is localized in the cytoplasm as well as the cell membrane [26]. The cells were incubated with 60  $\mu$ M of (6) for 48 h and visualized under the microscope using the mCherry filter set (Figure 5) [19].

In both cell lines, incubation with compound (6) led to the appearance of localized fluorescence (Figure 5), whereas no fluorescence was witnessed in the control cells. Further colocalization experiments utilizing (6), in combination with immunocytochemistry methods, are in progress to elucidate the exact nature of the observed fluorescence and to ascertain the specific binding to GP in a cellular environment.

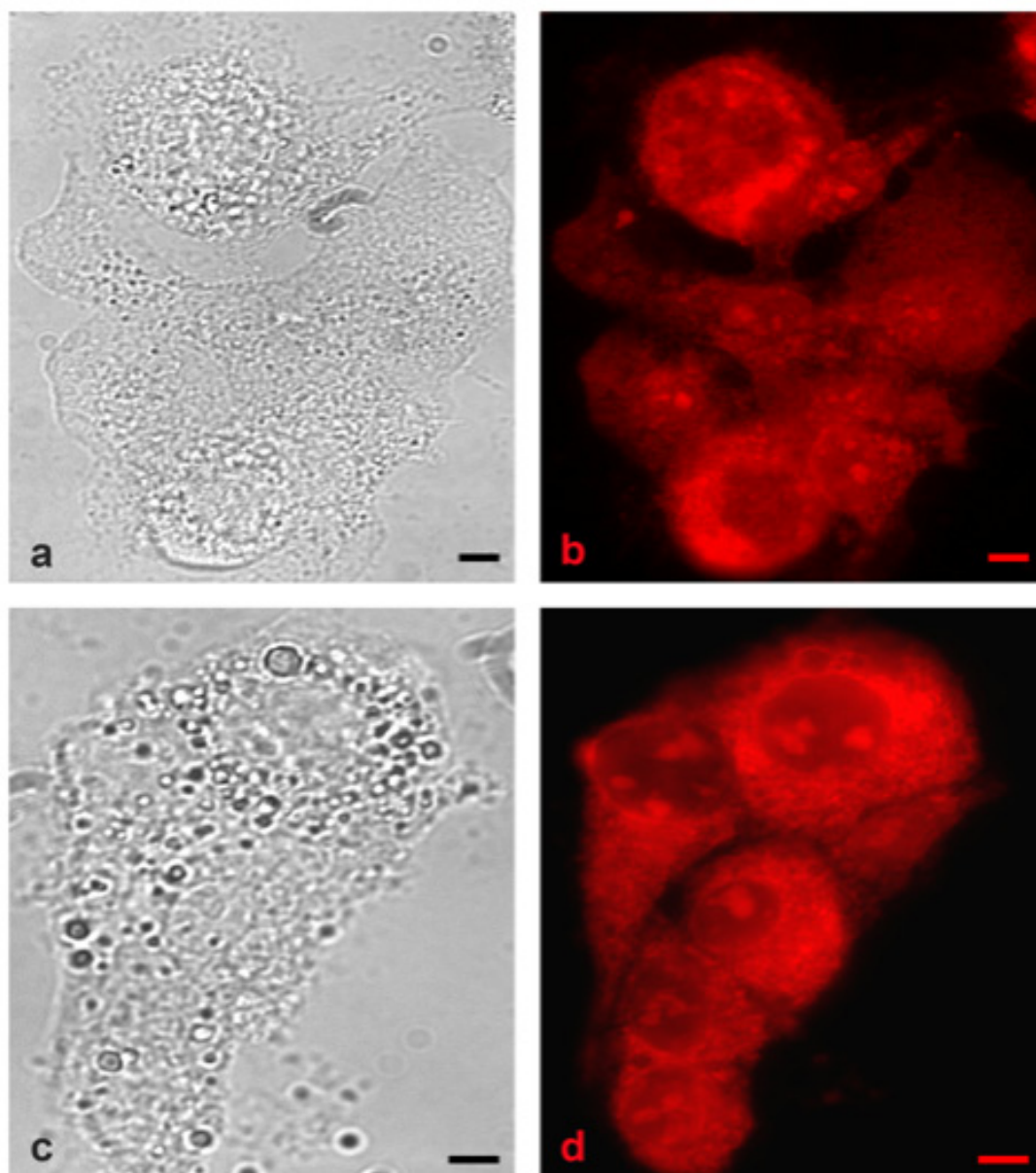


**Figure 5.** (a) A-431 cells under brightfield view, (b) A-431 cell fluorescence with mCherry filter set, (c) Hep2G cells under brightfield view, and (d) Hep2G cells' fluorescence with the mCherry filter. Both cell lines were incubated with 60  $\mu\text{M}$  of compound (6) for 48 h before acquisition of the above pictures.

### 3. Materials and Methods

All reagents, solvents, cell lines, cell culture media, and reagents were purchased from commercial sources and used without further purification. All reactions were carried out under an argon atmosphere on a magnetic stirrer and monitored by thin-layer chromatography. Compounds were purified by flash chromatography on 40–60  $\mu\text{m}$ , 60  $\text{\AA}$  silica gel. NMR measurements were performed with a Varian Mercury 200 Nuclear Magnetic Resonance Spectrometer (at 200 MHz for  $^1\text{H}$  and at 50 MHz for  $^{13}\text{C}$ ). Chemical shifts are given in ppm and were referenced on residual solvent peaks. Coupling constants were

measured in Hz. High-resolution mass spectrometry experiments were carried out in a Q-TOF Bruker MaXis Impact HR-Mass Spectrometer. 6-dimethylamino-2-naphthaldehyde (**1**) [20,21] and 2,3,4,6-tetra-*O*-acetyl- $\beta$ -D-glucopyranosylamine (**4**) [23,24] were synthesized by previously reported procedures.

Absorption spectra were acquired on a Shimadzu UV-Vis-NIR 3600 spectrophotometer, and excitation spectra were acquired on a Shimadzu RF-5301PC spectrofluorometer, utilizing a matched set of dual-path cuvettes. Britton Robinson universal buffers (BRB) were used for variable pH experiments and were prepared as described [27]. RMGP was isolated from rabbit skeletal muscle and its potency was assayed according to previously established protocols [28,29]. Measurements involving RMGP were performed in aqueous buffers (assay buffer), consisting of  $\beta$ -glycerophosphate (2.5 mM), 2-mercaptoethanol (2.5 mM), and EDTA (0.05 mM) for the first set of experiments, and the same buffer was used without inclusion of 2-mercaptoethanol for the second (successful) set of experiments described.

For the fluorescence microscopy experiments, both HepG2 and A431 cell lines were used. Cells were cultured as monolayers in Dulbecco's Modified Eagle's Medium (DMEM) medium supplemented with 10% (*v/v*) fetal bovine serum (FBS), 100 U/mL penicillin, and 100  $\mu$ g/mL streptomycin and were grown in 60 mm tissue culture dishes in a humidified 5% CO<sub>2</sub> atmosphere at 37 °C. Cells in their log phase of growth were harvested, counted, and seeded ( $4 \times 10^4$  cells/well in 250  $\mu$ L DMEM containing 10% FBS) in 8-well plates ( $\mu$ -Slide 8 well, IBIDI GMBH). After 24 h of incubation to allow cell attachment, the synthetic phosphorylase inhibitor (**6**) was added to a final concentration of 60  $\mu$ M and cells were incubated for 48 h before observation. Two replicates were set up in each experiment.

Before observing the cells on a Zeiss Axio Observer Z1 inverted microscope equipped with proper filters and the ZEN Blue software, the culture medium was discarded and attached cells were washed twice with isotonic phosphate buffered saline (PBS) solution. For visualization of compound (**6**), a 538–562 nm band-pass excitation filter was used, and the fluorescence was observed in the range of 570–640 nm through the red mCherry filter.

(*E*)-2-Cyano-3-(6-dimethylamino)-2-naphthylacrylic acid (**2**): to a solution of 6-dimethylamino-2-naphthaldehyde (**1**) (409 mg, 2.05 mmol) in 4.2 mL of anhydrous MeCN, were added cyanoacetic acid (266 mg, 3.1 mmol) and piperidine (230  $\mu$ L, 2.3 mmol). The mixture was refluxed for 16 h and decanted into a 1:1 1M HCl ice mixture. The settling solid was filtered, washed three times with deionized water, and dried under reduced pressure, to yield 491 mg (90%) of spectroscopically pure acid (**2**) as a brown powder. <sup>1</sup>H NMR (200 MHz, DMSO-*d*<sub>6</sub>):  $\delta$  8.30 (d, *J* = 2.3 Hz, 1H), 8.28 (s, 1H), 8.07 (dd, *J* = 8.9, 1.8 Hz, 1H), 7.80 (d, *J* = 9.2 Hz, 1H), 7.72 (d, *J* = 8.9 Hz, 1H), 7.26 (dd, *J* = 9.1, 2.5 Hz, 1H), 6.94 (d, *J* = 2.4 Hz, 1H), 3.08 (s, 6H). <sup>13</sup>C NMR (200 MHz, DMSO-*d*<sub>6</sub>):  $\delta$  164.2, 154.4, 150.6, 137.3, 135.2, 130.7, 126.7, 124.9, 124.8, 124.4, 117.2, 116.6, 104.9, 98.8, 39.9 (2C). HRMS [*M* - *H*]<sup>-</sup>: calculated for C<sub>16</sub>H<sub>13</sub>N<sub>2</sub>O<sub>2</sub><sup>-</sup> 265.0983; found 265.0965.

(*E*)-2-Cyano-3-(6-(dimethylamino)naphthalen-2-yl)-*N*-( $\beta$ -D-glucopyranosyl)acrylamide (**6**): a solution of acid (**2**) (267 mg, 1.00 mmol) in 2 mL of anhydrous DCM was cooled in an ice bath. A drop of DMF and oxalyl chloride (180  $\mu$ L, 2.09 mmol) were added dropwise. The mixture was brought to room temperature and stirred for a further 2 h. Volatiles were removed under reduced pressure. The residue was dissolved in 5 mL of anhydrous DCM and added dropwise to an ice-cooled solution of 2,3,4,6-tetra-*O*-acetyl- $\beta$ -D-glucopyranosylamine (**4**) (315 mg, 0.91 mmol) in 2 mL of anhydrous pyridine. The mixture was brought to room temperature and left to stir for 1 h, after which the reaction mixture was quenched by the addition of 1 mL of deionized water. The mixture was concentrated under reduced pressure, taken up in EtOAc and the organic portion was washed successively with 5% Na<sub>2</sub>CO<sub>3</sub> (1  $\times$  15 mL), deionized water (1  $\times$  15 mL), and brine (1  $\times$  10 mL),

separated, dried over anhydrous sodium sulfate, filtered through a silica plug, and concentrated. To the residue 7 M methanolic ammonia solution (7.5 mL) was added. After 24 h, the mixture was concentrated and purified by column chromatography to yield 150 mg of compound (**6**) (35% from (**2**)) as a bright orange powder.  $^1\text{H}$  NMR (200 MHz, DMSO- $d_6$ ):  $\delta$  8.81 (d,  $J$  = 8.7 Hz, 1H), 8.23 (s, 2H), 8.02 (dd,  $J$  = 8.6, 1.2 Hz, 1H), 7.85 (d,  $J$  = 9.2 Hz, 1H), 7.76 (d,  $J$  = 8.9 Hz, 1H), 7.29 (dd,  $J$  = 9.3, 2.4 Hz, 1H), 6.98 (d,  $J$  = 2.4 Hz, 1H), 5.09–5.01 (m, 2H), 4.95 (d,  $J$  = 4.9 Hz, 1H), 4.87 (t,  $J$  = 8.6 Hz, 1H), 4.56 (t,  $J$  = 5.7 Hz, 1H), 3.68 (dd,  $J$  = 11.7, 5.7 Hz, 1H), 3.46 (dd,  $J$  = 11.4, 5.3 Hz, 1H), 3.31–3.12 (m, 4H), 3.09 (s, 6H).  $^{13}\text{C}$  NMR (50 MHz, DMSO- $d_6$ ):  $\delta$  163.0, 151.2, 150.7, 137.2, 134.0, 130.7, 126.9, 125.1 (2C), 124.8, 117.4, 116.9, 105.1, 102.2, 80.6, 78.9, 77.3, 72.1, 70.0, 61.0, 40.1 (2C). HRMS  $[\text{M} + \text{Na}]^+$ : calculated for  $\text{C}_{22}\text{H}_{25}\text{N}_3\text{NaO}_6^+$  450.1641; found 450.1637.

#### 4. Conclusions

The first reported glucose derivative, (*E*)-2-cyano-3-(6-(dimethylamino)naphthalen-2-yl)-*N*-( $\beta$ -D-glucopyranosyl)acrylamide (**6**), bearing a molecular rotor moiety was synthesized and studied. The new compound was shown to exhibit molecular rotor fluorescence characteristics in viscous solutions as well as in complex with RMGP. Incubation of A-431 and Hep2G cancer cells led to the appearance of localized fluorescence in the red region, possibly indicating a selective binding of the new compound (**6**) to GP present in the cell. These studies correspond to a proof-of-concept, that a RMGP inhibitor with molecular rotor properties is feasible. Further studies are underway to develop further carbohydrate-based molecules with molecular rotor functionality, improved chemical stability, and strong binding to the catalytic site of GP. The aim is to access compounds with high fluorescence quantum yields and to finetune both the absorption and emission spectral values by varying substitutions on the aromatic system. This will allow coverage of the range of fluorescence filter-sets commonly used in fluorescence microscopy, and will extend applications to two-photon excitation, in order to probe living tissue.

**Supplementary Materials:** The following are available online at [www.mdpi.com/2673-4583/3/1/45/s1](http://www.mdpi.com/2673-4583/3/1/45/s1).

**Author Contributions:** Conceptualization, T.G.; methodology, K.F.M. and M.M.; investigation, K.F.M. and P.P.; writing—original draft preparation, T.G. and K.F.M.; writing—review and editing, T.G. and K.F.M.; visualization, T.G., P.P., K.F.M., and M.M.; supervision, T.G. and P.P.; project administration, T.G. and P.P.; funding acquisition, T.G. and K.F.M. All authors have read and agreed to the published version of the manuscript.

**Funding:** This research was co-financed by Greece and the European Union (European Social Fund—ESF) through the operational programme “Human Resources Development, Education and Lifelong Learning 2014–2020” in the context of the project “Synthesis and Study of Fluorescent Molecular Rotors as Cellular Probes for Enzymatic Function” (MIS 5048135).

**Institutional Review Board Statement:** Not applicable.

**Informed Consent Statement:** Not applicable.

**Data Availability Statement:** Additional data presented in this study are available in the Supplementary Material.

**Conflicts of Interest:** The authors declare no conflicts of interest.

#### References

1. World Health Organization. *Global Report on Diabetes*; World Health Organization: Geneva, Switzerland, 2016; ISBN 978-92-4-156525-7.
2. Praly, J.-P.; Vidal, S. Inhibition of Glycogen Phosphorylase in the Context of Type 2 Diabetes, with Focus on Recent Inhibitors Bound at the Active Site. *Mini-Rev. Med. Chem.* **2010**, *10*, 1102–1126, doi:10.2174/1389557511009011102.
3. Rousset, M.; Robine-Leon, S.; Dussaulx, E.; Chevalier, G.; Zweibaum, A. Glycogen Storage in Foetal and Malignant Epithelial Cells of the Human Colon. *Front. Gastrointest. Res.* **1979**, 80–85, doi:10.1159/000402288.

4. Lee, W.-N.P.; Guo, P.; Lim, S.; Bassilian, S.; Lee, S.T.; Boren, J.; Cascante, M.; Go, V.L.W.; Boros, L.G. Metabolic sensitivity of pancreatic tumour cell apoptosis to glycogen phosphorylase inhibitor treatment. *Br. J. Cancer* **2004**, *91*, 2094–2100, doi:10.1038/sj.bjc.6602243.
5. Schnier, J.B.; Nishi, K.; Monks, A.; Gorin, F.A.; Bradbury, E.M. Inhibition of glycogen phosphorylase (GP) by CP-91,149 induces growth inhibition correlating with brain GP expression. *Biochem. Biophys. Res. Commun.* **2003**, *309*, 126–134, doi:10.1016/S0006-291X(03)01542-0.
6. Favaro, E.; Harris, A.L. Targeting glycogen metabolism: A novel strategy to inhibit cancer cell growth? *Oncotarget* **2013**, *4*, 3–4, doi:10.18632/oncotarget.841.
7. Bak, L.K.; Walls, A.B. Astrocytic glycogen metabolism in the healthy and diseased brain. *J. Biol. Chem.* **2018**, *293*, 7108–7116, doi:10.1074/jbc.R117.803239.
8. Swanson, R.A. Brain glycogen—Vestigial no more. *Metab. Brain Dis.* **2015**, *30*, 251–253, doi:10.1007/s11011-014-9596-2.
9. Gimisis, T. Synthesis of N-Glucopyranosidic Derivatives as Potential Inhibitors that Bind at the Catalytic Site of Glycogen Phosphorylase. *Mini-Rev. Med. Chem.* **2010**, *10*, 1127–1138, doi:10.2174/1389557511009011127.
10. Mamais, M.; Degli Esposti, A.; Kouloumoundra, V.; Gustavsson, T.; Monti, F.; Venturini, A.; Chrysina, E.D.; Markovitsi, D.; Gimisis, T. A New Potent Inhibitor of Glycogen Phosphorylase Reveals the Basicity of the Catalytic Site. *Chem. A Eur. J.* **2017**, *23*, 8800–8805, doi:10.1002/chem.201701591.
11. Mamais, M.; Kouloumoundra, V.; Smyrli, E.; Grammatopoulos, P.; Chrysina, E.D.; Gimisis, T. Synthesis of N4-aryl- $\beta$ -D-glucopyranosylcytosines: A methodology study. *Tetrahedron Lett.* **2015**, *56*, 5549–5552, doi:10.1016/j.tetlet.2015.08.037.
12. Haidekker, M.A.; Theodorakis, E.A. Molecular rotors—fluorescent biosensors for viscosity and flow. *Org. Biomol. Chem.* **2007**, *5*, 1669–1678, doi:10.1039/b618415d.
13. Loutfy, R.O. Fluorescence probes for polymer free-volume. *Pure Appl. Chem.* **1986**, *58*, doi:10.1351/pac198658091239.
14. Haidekker, M.A.; Ling, T.; Anglo, M.; Stevens, H.Y.; Frangos, J.A.; Theodorakis, E.A. New fluorescent probes for the measurement of cell membrane viscosity. *Chem. Biol.* **2001**, *8*, 123–131, doi:10.1016/S1074-5521(00)90061-9.
15. Mallipattu, S.; Haidekker, M.; Von Dassow, P.; Latz, M.; Frangos, J. Evidence for shear-induced increase in membrane fluidity in the dinoflagellate *Lingulodinium polyedrum*. *J. Comp. Physiol. A* **2002**, *188*, 409–416, doi:10.1007/s00359-002-0315-9.
16. Pal, S.; Chakraborty, H.; Bandari, S.; Yahioğlu, G.; Suhling, K.; Chattopadhyay, A. Molecular rheology of neuronal membranes explored using a molecular rotor: Implications for receptor function. *Chem. Phys. Lipids* **2016**, *196*, 69–75, doi:10.1016/j.chemphyslip.2016.02.004.
17. Zhou, K.; Li, Y.; Peng, Y.; Cui, X.; Dai, J.; Cui, M. Structure–Property Relationships of Polyethylene Glycol Modified Fluorophore as Near-Infrared  $A\beta$  Imaging Probes. *Anal. Chem.* **2018**, *90*, 8576–8582, doi:10.1021/acs.analchem.8b01712.
18. Koo, J.Y.; Heo, C.H.; Shin, Y.-H.; Kim, D.; Lim, C.S.; Cho, B.R.; Kim, H.M.; Park, S.B. Readily Accessible and Predictable Naphthalene-Based Two-Photon Fluorophore with Full Visible-Color Coverage. *Chem. A Eur. J.* **2016**, *22*, 14166–14170, doi:10.1002/chem.201603496.
19. Parrello, D.; Mustin, C.; Brie, D.; Miron, S.; Billard, P. Multicolor Whole-Cell Bacterial Sensing Using a Synchronous Fluorescence Spectroscopy-Based Approach. *PLoS ONE* **2015**, *10*, e0122848, doi:10.1371/journal.pone.0122848.
20. Koelsch, F. 6-BROMO-2-NAPHTHOL. *Org. Synth.* **1940**, *20*, 18, doi:10.15227/orgsyn.020.0018.
21. Rao, A.S.; Kim, D.; Wang, T.; Kim, K.H.; Hwang, S.; Ahn, K.H. Reaction-based two-photon probes for mercury ions: Fluorescence imaging with dual optical windows. *Org. Lett.* **2012**, *14*, 2598–2601, doi:10.1021/ol3009057.
22. Gurrupu, S.; Jonnalagadda, S.K.; Alam, M.A.; Nelson, G.L.; Sneve, M.G.; Drewes, L.R.; Mereddy, V.R. Monocarboxylate transporter 1 inhibitors as potential anticancer agents. *ACS Med. Chem. Lett.* **2015**, *6*, 558–561, doi:10.1021/acsmedchemlett.5b00049.
23. Badía, C.; Souard, F.; Vicent, C. Sugar–Oligoamides: Synthesis of DNA Minor Groove Binders. *J. Org. Chem.* **2012**, *77*, 10870–10881, doi:10.1021/jo302238u.
24. Van Ameijde, J.; Albada, H.B.; Liskamp, R.M.J. A convenient preparation of several N-linked glycoamino acid building blocks for efficient solid-phase synthesis of glycopeptides. *J. Chem. Soc. Perkin Trans. 1* **2002**, *2*, 1042–1049, doi:10.1039/b201296k.
25. Pels, K.; Dickson, P.; An, H.; Kodadek, T. DNA-Compatible Solid-Phase Combinatorial Synthesis of  $\beta$ -Cyanoacrylamides and Related Electrophiles. *ACS Comb. Sci.* **2018**, *20*, 61–69, doi:10.1021/acscmbosci.7b00169.
26. Uhlén, M.; Björling, E.; Agaton, C.; Szgyarto, C.A.K.; Amini, B.; Andersen, E.; Andersson, A.C.; Angelidou, P.; Asplund, A.; Asplund, C.; et al. A human protein atlas for normal and cancer tissues based on antibody proteomics. *Mol. Cell. Proteom.* **2005**, *4*, 1920–1932, doi:10.1074/mcp.M500279-MCP200.
27. Britton, H.T.S.; Robinson, R.A. CXC VIII. — Universal buffer solutions and the dissociation constant of veronal. *J. Chem. Soc.* **1931**, 1456–1462, doi:10.1039/JR9310001456.
28. Oikonomakos, N.G.; Kontou, M.; Zographos, S.E.; Watson, K.A.; Johnson, L.N.; Bichard, C.J.F.; Fleet, G.W.J.; Acharya, K.R. N-acetyl- $\beta$ -D-glucopyranosylamine: A potent T-state inhibitor of glycogen phosphorylase. A comparison with  $\alpha$ -D-glucose. *Protein Sci.* **1995**, *4*, 2469–2477, doi:10.1002/pro.5560041203.
29. Saheki, S.; Takeda, A.; Shimazu, T. Assay of inorganic phosphate in the mild pH range, suitable for measurement of glycogen phosphorylase activity. *Anal. Biochem.* **1985**, *148*, 277–281, doi:10.1016/0003-2697(85)90229-5.